*Thermochimica Acta*, 145 (1989) 331–352
Elsevier Science Publishers B.V., Amsterdam – Printed in The Netherlands

# THERMAL DEGRADATION OF CELLULOSE, CELLULOSE THIOPHOSPHATE AND ITS COMPLEXES WITH TRANSITION-METAL CATIONS

RAMA KANT KAUSHIK, I.S. GUR and HARI L. BHATNAGAR *
*Department of Chemistry, Kurukshetra University, Kurukshetra 132119 (India)*

(Received 17 November 1988)

## ABSTRACT

Complexes of cellulose thiophosphate (CSP) with transition metals such as Ti(III), V(IV), Cr(III), Mn(II), Fe(II), Co(II), Ni(II), Cu(II), Zn(II), Zr(IV), Mo(VI), Cd(II) and La(III) have been characterised by UV–visible spectroscopy and elemental analysis. The thermal behaviour of cotton fibres, CSP and its metal complexes in air have been studied by differential thermal analysis (DTA), thermogravimetric (TG) and differential thermal analysis (DTG) techniques from ambient temperature to 800 °C. From the resulting data, the energies of activation and the frequency factors were calculated for various stages of thermal degradation using the method of Broido. The IR and ESR spectra of the chars were used in elucidating the mechanism of the oxidative thermal degradation of CSP and its metal complexes.

## INTRODUCTION

Cotton fibre contains mainly cellulose (93.0%) [1]. The properties of cellulose and the modified celluloses have been extensively studied and reviewed [2–4]. The behaviour of some of these derivatives toward oxidation, thermal treatment, pyrolysis, hydrolysis and photodegradation have also been reported [5–9].

The purpose of the present studies was to investigate the effect of phosphorus in combination with sulphur, chlorine, nitrogen and transition metals on the oxidative thermal degradation of cotton fibres in air. It is known that the primary role of these elements is to change the decomposition process [10,11] occurring from ambient temperature to 800 °C.

## EXPERIMENTAL

The following samples were selected for the present studies: (1) cotton fibres dried to a constant weight at 60 °C; (2) cellulose thiophosphate (CSP)

---

* Author to whom correspondence should be addressed.

TABLE 1

Analytical data for cotton fibre, CSP and metal complexes of CSP

| Sample No. | Compound/complex | Colour | P (%) | S (%) | Cl (%) | N (%) | Metal (%) |
|---|---|---|---|---|---|---|---|
| 1 | Cotton fibre | Snow white | – | – | – | – | – |
| 2 | CSP | Light brown | 6.25 | 1.38 | 1.58 | 1.02 | – |
| 3 | Ti(III)–CSP | Light brown | 5.53 | 1.62 | 1.37 | 0.68 | 0.04 |
| 4 | V(IV)–CSP | Light green | 5.62 | 1.47 | 1.55 | 1.01 | 0.009 |
| 5 | Cr(III)–CSP | Bluish green | 6.16 | 1.41 | 1.28 | 0.84 | 1.17 |
| 6 | Mn(III)–CSP | Light brown | 5.89 | 1.55 | 1.33 | 0.92 | 0.33 |
| 7 | Fe(II)–CSP | Brownish yellow | 5.86 | 1.29 | 1.26 | 0.89 | 0.83 |
| 8 | Co(II)–CSP | Light violet | 6.60 | 1.91 | 1.70 | 0.96 | 0.24 |
| 9 | Ni(II)–CSP | Light brown | 6.51 | 1.62 | 1.58 | 0.79 | 0.57 |
| 10 | Cu(II)–CSP | Bluish green | 4.62 | 1.12 | 1.49 | 0.85 | 1.84 |
| 11 | Zn(II)–CSP | Light brown | 6.21 | 1.86 | 1.57 | 0.82 | 1.34 |
| 12 | Zr(IV)–CSP | Light brown | 5.26 | 1.29 | 1.28 | 0.93 | 0.68 |
| 13 | Mo(VI)–CSP | Light brown | 5.91 | 1.11 | 1.45 | 0.76 | 0.02 |
| 14 | Cd(II)–CSP | Light yellow | 5.20 | 1.39 | 1.36 | 0.87 | 0.70 |
| 15 | La(III)–CSP | Light brown | 5.70 | 1.30 | 1.09 | 0.72 | 0.25 |

prepared [12,13] by treating mercerised cotton fibres with phosphorus thiochloride in pyridine at 95 °C for 6 h and dried at 60 °C; (3–15) Ti(III), V(IV), Cr(III), Mn(II), Fe(II), Co(II), Ni(II), Cu(II), Zn(II), Zr(IV), Mo(VI), Cd(II) and La(III) complexes of CSP, respectively. Samples (3–15) were prepared by treating 2.0 g of CSP in each instance with 5% aqueous solutions of $TiCl_3$, $VOSO_4 \cdot 5H_2O$, $Cr_2(SO_4)_3 \cdot xH_2O$, $MnSO_4 \cdot H_2O$, $FeSO_4 \cdot 7H_2O$, $CoSO_4 \cdot H_2O$, $NiSO_4 \cdot 6H_2O$, $CuSO_4 \cdot 5H_2O$, $ZnSO_4 \cdot 7H_2O$, $Zr(SO_4)_2 \cdot 4H_2O$, $(NH_4)_6 \cdot Mo_7O_{24} \cdot 4H_2O$, $CdCl_2 \cdot 5H_2O$ and $LaCl_3 \cdot xH_2O$, respectively, at room temperature for 48 h with stirring after an interval of 4 h. In each case the product was washed repeatedly with distilled water until the effluent water was free from metal salt and then with a solution of detergent and 4% $NaHCO_3$ at the boiling point of the solution for 3 h. Each sample was kept at pH 5 for 1 h and, after washing with distilled water, kept at pH 10 for a further 1 h. After a thorough washing with distilled water, the samples were dried at 60 °C. The sulphur content of each CSP–metal complex (Table 1) was found to be less than the phosphorus content. This indicates that, under the vigorous condition of boiling for 3 h in soap-soda solution, there may be a partial replacement of S by O in the phosphate ester group.

### *Elemental analysis*

The elemental analysis of phosphorus, sulphur, chlorine and transition metals was made using X-ray fluorescence spectrometry and nitrogen was determined using the Kjeldahl method. The results are reported in Table 1.

### *UV-visible spectral analysis*

The reflectance UV–visible spectra of CSP and the CSP–metal complexes were recorded using a Cary Model 1711 diffuse-reflectance accessory attached to a Cary 17D spectrophotometer (Varian, Palo Alto, CA, U.S.A.). Magnesium carbonate was used as reference.

### *Thermal analysis*

Differential thermal analysis (DTA), thermogravimetry (TG) and differential thermogravimetry (DTG) were carried out using a NETZSCH STA 409 Thermal Analyser. The DTA, TG and DTG curves were obtained in a dynamic air medium from ambient temperature to 800 ° C at a scanning rate of $10\,^{\circ}\mathrm{C\ min}^{-1}$.

### *Infrared spectral analysis*

For the IR studies, KBr discs containing 2% of the charred products of CSP and the CSP–metal complexes were prepared and the spectra recorded on a Beckman IR-20 spectrophotometer. The charred samples were prepared by heating the compounds to the desired temperature.

### *ESR analysis*

The electron spin resonance (ESR) spectra of cotton fibre, CSP and the CSP complexes of Fe(II) and Cu(II) were recorded on a Varian E-112 ESR spectrometer operating at 9.45 GHz with a field modulation of 100 kHz. Charred sample (100 mg) was used for each measurement. The 1,1-diphenyl-2-picryl hydrazyl (DPPH) signal was used as the *g*-value standard.

### *Characterisation of samples*

CSP was characterised by its IR spectrum and the CSP–metal complexes by their reflectance UV–visible spectra.

It has been shown that various transition-metal ions can form complexes with cellulose phosphate and cellulose ammonium phosphate [13,14]. CSP also forms complexes with the transition-metal ions. A general reaction between CSP and bivalent metal cations for the formation of complexes can be written as shown below [13] where M is a transition metal.

The reflectance UV–visible spectra of the complexes are discussed below.

The Ti(III) complex of CSP showed a broad band located at about 493 nm. This may be attributed to the transition $^2E_g \leftarrow {}^2T_{2g}$ [15]. The V(IV) complex exhibited wide weak bands at 581 and 391 nm, which may be due

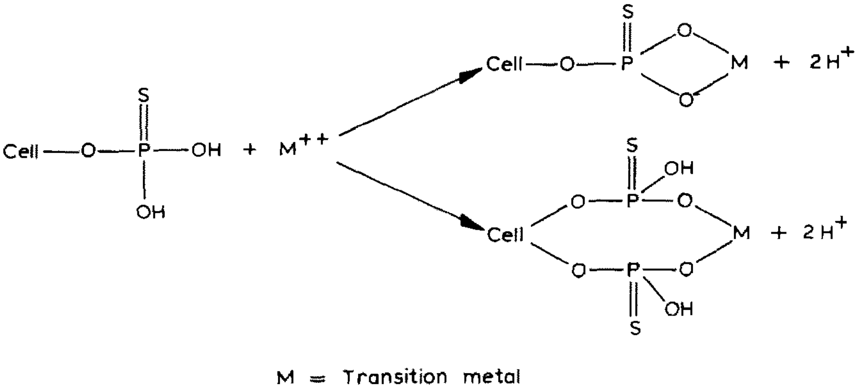

to the spin-allowed transitions $^3T_{1g}(F) \rightarrow {}^3T_{2g}(F)$ and $^3T_{1g}(F) \rightarrow {}^3A_{2g}(F)$, respectively.

The Cr(III) complex of CSP showed two absorption bands around 590 and 416 nm, which are assigned to the $^4A_{2g}(F) \rightarrow {}^4T_{2g}(F)$ $(\nu_1)$ and

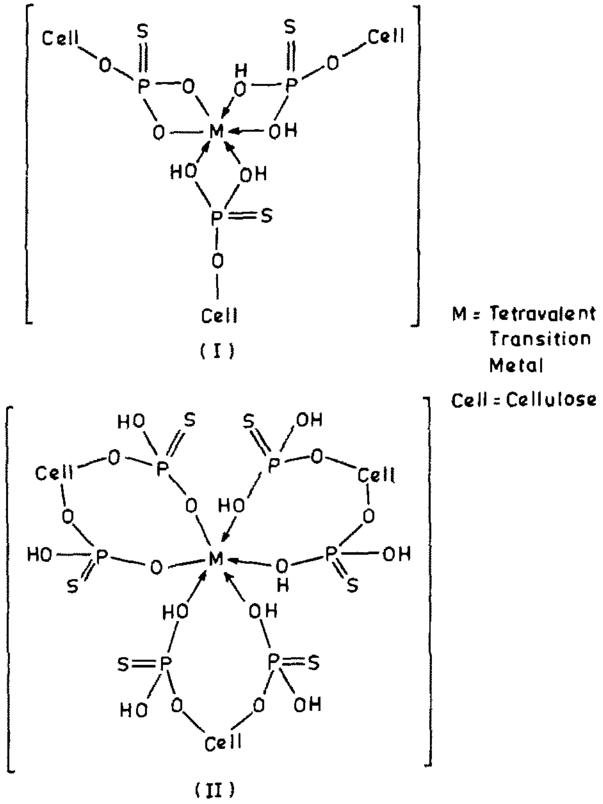

Scheme 1. Two possible structures of the metal–CSP complexes.

$^4A_{2g}(F) \rightarrow {}^4T_{1g}(F)$ ($\nu_2$) transitions, respectively, suggesting an octahedral structure of the complex [16]. The Fe(II) complex exhibited an absorption band at 480 nm, which is due to the spin-allowed transition $^5T_{2g} \rightarrow {}^5E_g$ for octahedral complexes [17].

The Co(II) complex showed a band at 625 nm and another very weak band at 500 nm. These may be due to $^4T_{1g} \rightarrow {}^4A_{2g}(F)$ and $^4T_{1g} \rightarrow {}^4T_{1g}(P)$ transitions, respectively, again for octahedral complexes [16].

The Cu(II) complex showed a sharp band at 725 nm, which can be attributed to the $^2E_g \rightarrow {}^2T_{2g}$ transition. This band is typical of Cu(II) ions in a tetragonally distorted octahedron [18].

The Mn(II), Ni(II), Zn(II), Zr(IV), Mo(VI), Cd(II) and La(III) complexes did not absorb in the UV–visible region. However, as the octahedral nature of metal complexes of CSP has been confirmed for Cr(III), Fe(II) and Co(II) complexes, it is assumed that the other metal ions also form octahedral complexes. Two possible structures of the metal complexes of CSP are shown in Scheme 1 [13]. Of these two structures, structure **I** is more probable; structure **II**, being a large-membered ring, would be less stable.

## RESULTS AND DISCUSSION

It is known that at lower temperatures, i.e. below 300 °C, degradation of cellulose takes place gradually through dehydration, rearrangement, formation of carboxyl and carbonyl groups, evolution of $CO_2$ and CO, and formation of carbonaceous char [19,20]. At temperatures above 300 °C, rapid volatilization accompanied by the formation of intractable tars and carbonaceous residue occurs. The major product in cellulose tar is laevoglucosan [21,22] (1,6-anhydro-β-D-glucopyranose) which may be obtained in yields of 40% or more together with polymeric materials, which are similar to the condensation products of laevoglucosan and the apparently randomly linked oligosaccharides [23].

The DTA, TG and DTG curves of (1) cotton fibres, (2) CSP and (3–15) complexes of CSP were obtained in a dynamic air medium. The curves for samples 1, 2 and 7 are shown in Figs. 1–3 (the curves for samples 3–6 and 8–15 are not shown but can be obtained from the authors on request). The peak temperatures for the various endotherms and exotherms of the DTA for all the compounds investigated are given in Table 2.

The DTA curve of cotton fibres (Fig. 1) showed the usual features discussed previously [24]. The DTA curves of CSP and its metal derivatives are entirely different from that of cotton fibres.

During the process of thiophosphorylation of cellulose, chlorodeoxycellulose is also formed. Therefore, chlorine plays a significant role in altering the thermal degradation. It has been shown by Shafizadeh et al. [25] that in the thermal degradation of 6-chlorodeoxycellulose, the initial reaction begins

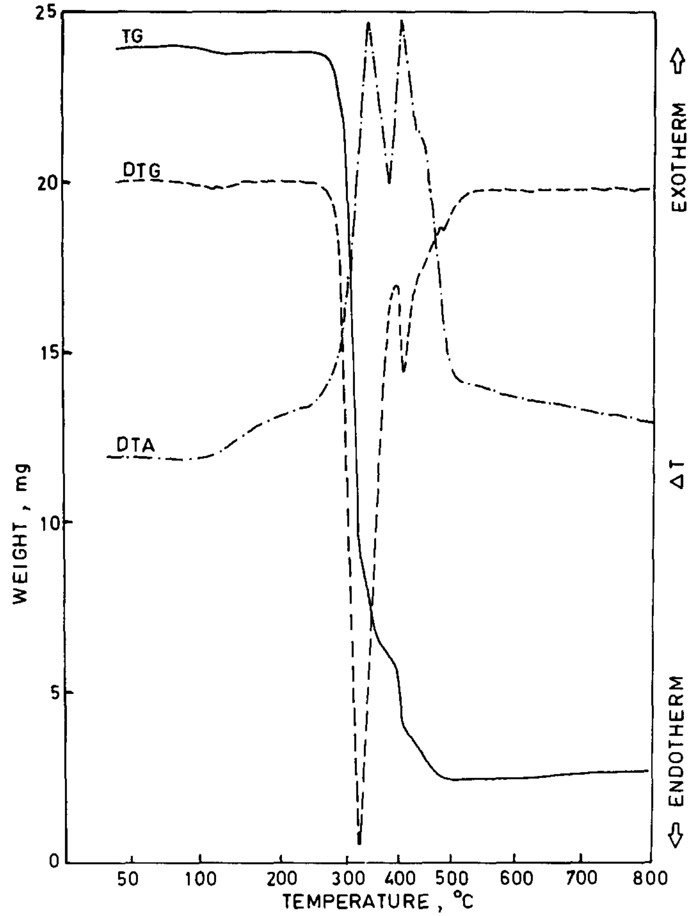

Fig. 1. Thermal analysis of cotton fibre in air.

with dehydrohalogenation at around 200 °C and the hydrogen chloride released then catalyses a series of heterolytic reactions.

CSP forms complexes with transition-metal cations and chlorodeoxycellulose does not participate in this process. Therefore, the main stress is reasonably only on the thermal properties of CSP and its metal complexes.

In the case of CSP, a large endotherm peaking at 105 °C appears which corresponds to dethiophosphorylation, dehydrohalogenation and dehydration [13]. The endotherm is followed by four exotherms peaking at 250, 300, 438 and 770 °C. The first exotherm represents the decomposition process leading to char formation [13]. The exotherms with peak temperatures at 300 and 438 °C correspond to the oxidation of the aliphatic and aromatic components of char, respectively, and the peak at 770 °C to the decomposition of polythiophosphates [13].

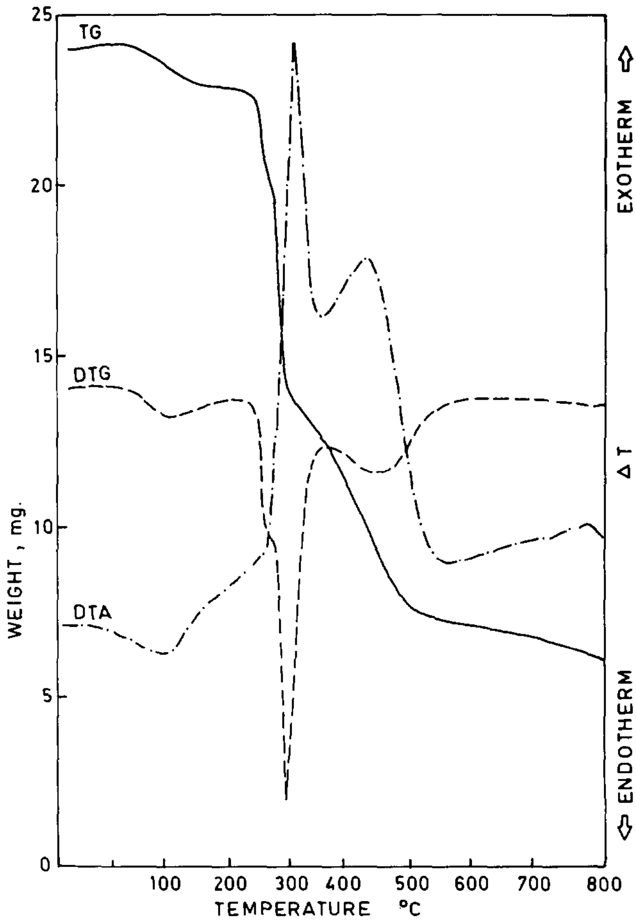

Fig. 2. Thermal analysis of CSP in air.

The metal complexes of CSP, in general, show one endotherm and four exotherms (Table 2). The endotherm is due to the dehydration, the dehydrohalogenation and the release of metal thiophosphates. The metal thiophosphates may polymerize at higher temperatures. The exotherms are due to the decomposition, the oxidative thermal decomposition of the alicyclic and aromatic components of char, and the decomposition of metal thiophosphates (or their polymers), respectively. In all the metal complexes the endotherm lies at higher temperatures than in the case of CSP. The first endotherm which represents the decomposition stage shows an increase in decomposition temperature in all the complexes except for those with Cr(III), Cu(II), Zr(IV) and Cd(II) (Table 2). The nature of the second and the third exotherms is the same with slight variations in the peak temperatures in all the complexes except in Cu(II). In the case of Cu(II), the second exotherm is at a somewhat lower temperature as compared with the other

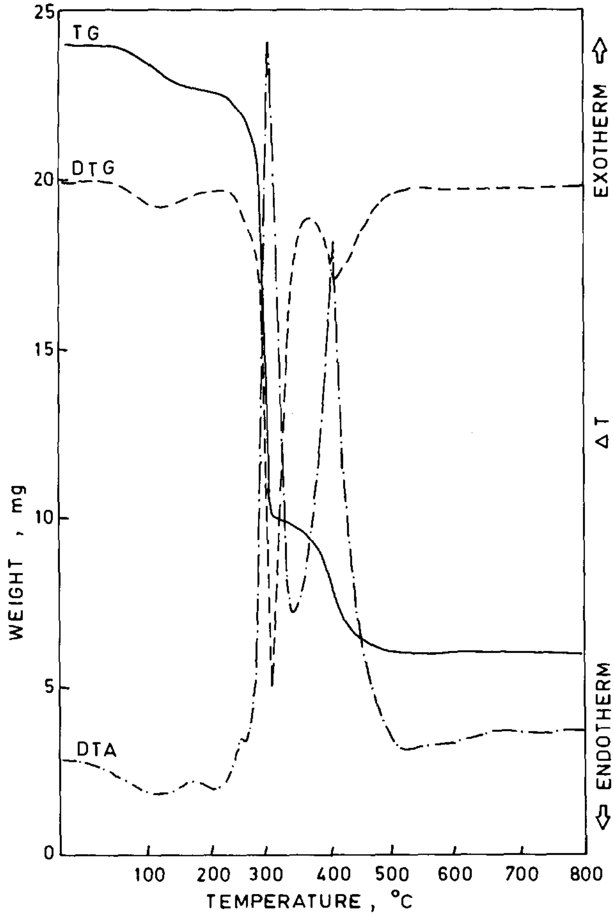

Fig. 3. Thermal analysis of the Fe(II)–CSP complex in air.

metal complexes. The last exotherm, which is possibly due to the decomposition of metal thiophosphate, shows considerable variation between the different complexes. In the case of the Cr(III), Mn(II), Zr(IV) and Cd(II) complexes this peak is missing, indicating that the decomposition of these compounds occurs at comparatively higher temperatures.

The kinetic parameters for the various stages of thermal degradation were determined from the TG curves using the following equation, described by Broido [26],

$$\ln\left(\ln\frac{1}{y}\right) = -\frac{E_a}{R}\frac{1}{T} + \ln\left(\frac{R}{E_a}\frac{Z}{R_H}T_m^2\right)$$

where $y$ is the fraction of the number of initial molecules not yet decomposed, $T_m$ is the temperature of maximum reaction rate, $R_H$ is the rate of heating, and $Z$ is the frequency factor.

TABLE 2

Peak temperatures in the DTA thermograms for cotton fibres, CSP and metal complexes of CSP in air

| Sample No. | Compound/complex | DTA curve, peak temperature (° C) | | | Nature of peak |
|---|---|---|---|---|---|
| | | Initiation | Maxima | Termination | |
| 1 | Cotton fibre | 240 | 340 | 385 | Exo, large |
| | | 385 | 408 | 432 | Exo, large |
| | | 432 | 455 | 520 | Exo, large |
| 2 | CSP | – | 105 | 200 | Endo, large |
| | | 200 | 250 | 256 | Exo, large |
| | | 256 | 300 | 362 | Exo, large |
| | | 362 | 438 | 570 | Exo, large |
| | | 570 | 770 | 850 | Exo, large |
| 3 | Ti(III)–CSP | – | 120 | 190 | Endo, large |
| | | 190 | 260 | 266 | Exo, large |
| | | 266 | 315 | 400 | Exo, large |
| | | 400 | 452 | 550 | Exo, large |
| | | 585 | 670 | – | Exo, large |
| 4 | V(IV)–CSP | – | 116 | 215 | Endo, large |
| | | 235 | 260 | 266 | Exo, large |
| | | 266 | 302 | 345 | Exo, large |
| | | 345 | 422 | 560 | Exo, large |
| | | 605 | 690 | – | Exo, large |
| 5 | Cr(III)–CSP | – | 118 | 200 | Endo, large |
| | | 200 | 248 | 255 | Exo, large |
| | | 255 | 292 | 338 | Exo, large |
| | | 442 | 572 | – | Exo, large |
| 6 | Mn(II)–CSP | – | 115 | 200 | Endo, large |
| | | 200 | 265 | 270 | Exo, large |
| | | 270 | 310 | 350 | Exo, large |
| | | 350 | 415 | 520 | Exo, large |
| | | 520 | 560 | 700 | Exo, large |
| 7 | Fe(II)–CSP | – | 120 | 172 | Endo, large |
| | | 212 | 255 | 264 | Exo, large |
| | | 264 | 315 | 345 | Exo, large |
| | | 345 | 405 | 530 | Exo, large |
| | | 545 | 675 | 720 | Exo, large |
| 8 | Co(II)–CSP | – | 120 | 180 | Endo, large |
| | | 215 | 260 | 266 | Exo, large |
| | | 266 | 302 | 345 | Exo, large |
| | | 345 | 422 | 560 | Exo, large |
| | | 605 | 690 | 785 | Exo, large |
| 9 | Ni(II)–CSP | – | 120 | 210 | Endo, large |
| | | 210 | 255 | 265 | Exo, large |
| | | 265 | 300 | 330 | Exo, large |
| | | 415 | 435 | 568 | Exo, large |
| | | 620 | 720 | 785 | Exo, large |

TABLE 2 (continued)

| Sample No. | Compound/complex | DTA curve, peak temperature (°C) | | | Nature of peak |
|---|---|---|---|---|---|
| | | Initiation | Maxima | Termination | |
| 10 | Cu(II)–CSP | – | 128 | 185 | Endo, large |
| | | 185 | 200 | 218 | Exo, large |
| | | 218 | 285 | 330 | Exo, large |
| | | 330 | 400 | 490 | Exo, large |
| | | 490 | 540 | 600 | Exo, large |
| | | 680 | 764 | – | Exo, large |
| 11 | Zn(II)–CSP | – | 118 | 200 | Endo, large |
| | | 235 | 300 | 352 | Exo, large |
| | | 352 | 425 | 560 | Exo, large |
| | | 566 | 795 | – | Exo, large |
| 12 | Zr(IV)–CSP | – | 120 | 200 | Endo, large |
| | | 200 | 245 | 255 | Exo, large |
| | | 255 | 305 | 350 | Exo, large |
| | | 350 | 406 | 520 | Exo, large |
| | | 520 | 565 | 615 | Exo, large |
| 13 | Mo(VI)–CSP | – | 115 | 225 | Endo, large |
| | | 225 | 250 | 264 | Exo, large |
| | | 264 | 300 | 350 | Exo, large |
| | | 350 | 430 | 555 | Exo, large |
| | | 605 | 705 | – | Exo, large |
| 14 | Cd(II)–CSP | – | 103 | 200 | Endo, large |
| | | 200 | 235 | 240 | Exo, large |
| | | 240 | 306 | 360 | Exo, large |
| | | 360 | 428 | 535 | Exo, large |
| | | 535 | 570 | 620 | Exo, large |
| 15 | La(III)–CSP | – | 118 | 200 | Endo, large |
| | | 200 | 255 | 260 | Exo, large |
| | | 260 | 310 | 355 | Exo, large |
| | | 355 | 421 | 540 | Exo, large |
| | | 540 | 605 | 630 | Exo, large |
| | | 630 | 705 | – | Exo, large |

Plots of $\ln(\ln 1/y)$ versus $1/T$ for the various stages of the thermal degradation of compounds 1–15 are shown in Figs. 4–6. The activation energies $E_a$ and frequency factors $Z$ determined from the slopes and intercepts, respectively, of these plots are given in Tables 3–5.

Table 3 gives the activation energies and frequency factors for the first stage of the thermal degradation of cotton fibres, CSP and the CSP–metal complexes. The small weight loss below 100 °C is due to the loss of the sorbed moisture and was neglected. Cotton fibres show a weight loss of 6.35% in the temperature range 250–285 °C caused by a dehydration reac-

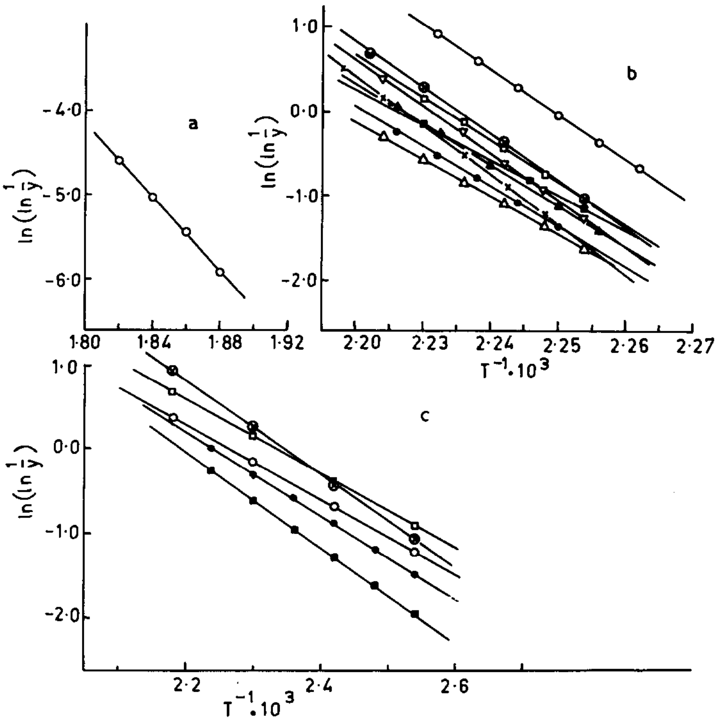

Fig. 4. Plots of ln(ln 1/$y$) vs. $T^{-1} \times 10^3$ using the Broido equation. a, Cotton fibre; b, CSP (○), Ti(III) (□), V(IV) (●), Cr(III) (△), Mn(II) (▽), Fe(II) (▲), Co(II) (■), Ni(II) (⊗) nd Zn(II) (×); c, Cu(II) (●), Zr(IV) (○), Mo(VI) (□), Cd(II) (■) and La(III) (⊗) complexes of CSP for the first stage of the thermal degradation in air.

tion. The activation energy for this stage is found to be 178.8 kJ mol$^{-1}$. In the case of CSP, about 2.8% of its weight is lost in the temperature range 100–180 °C primarily owing to dethiophosphorylation, dehydrohalogenation and dehydration reactions. The activation energy for this stage is 43.5 kJ mol$^{-1}$. This weight loss corresponds to the endotherm in the DTA curve of CSP below 200 °C. In the case of the CSP–metal complexes, similar weight losses are observed. The activation energies of the metal complexes of CSP for this stage are in the range 33.5–48 kJ mol$^{-1}$. The weight losses for samples 3–15 corresponding to the respective temperature ranges are 3.0, 2.4, 2.4, 2.4, 2.7, 3.0, 3.2, 2.6, 3.4, 1.5, 1.7, 2.0 and 2.6%, respectively. The DTG maxima of all the complexes lie around 120 °C (Table 3).

Table 4 gives the activation energies and frequency factors for the second stage of the thermal degradation of cellulose, CSP and the CSP–metal complexes. For cotton fibres, a weight loss of 58.05% occurs in the temperature range 285–330 °C. The activation energy for this temperature range is 256.9 kJ mol$^{-1}$. The data in Table 4 show that, in the case of CSP and its complexes, there is a decrease in the decomposition temperature to

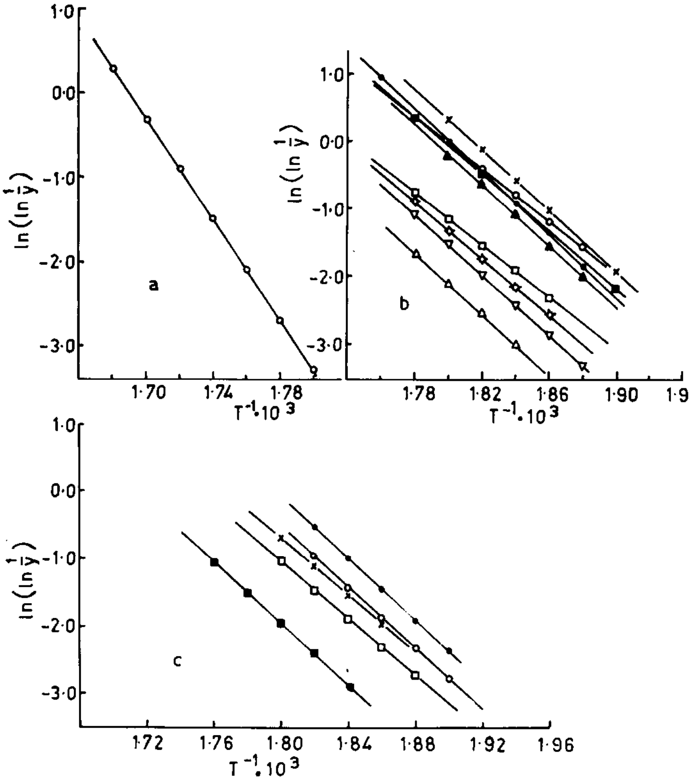

Fig. 5. Plots of ln(ln 1/$y$) vs. $T^{-1} \times 10^3$ using the Broido equation. a, Cotton fibre; b, CSP (●), Ti(III) (■), V(IV) (▲), Cr(III) (×), Mn(II) (□), Fe(II) (◇), Co(II) (△), Ni(II) (○) and Zn(II) (▽); c, Cu(II) (○), Zr(IV) (×), Mo(VI) (●), Cd(II) (□) and La(III) (■) complexes of CSP for the second stage of the thermal degradation in air.

240–300 °C and in the activation energies to 158–190 kJ mol$^{-1}$. CSP has an activation energy of 191.8 kJ mol$^{-1}$ for the decomposition stage with a weight loss of 33.5%. For the metal complexes of CSP, there is a decrease in the activation energy (158–190 kJ mol$^{-1}$) for all complexes except that with Mo(VI) for which the energy of activation is 192.1 kJ mol$^{-1}$.

Weight losses for the second stage for samples 3–15 are 35.25, 45.63, 40.9, 53.22, 52.6, 46.2, 31.13, 54.56, 38.3, 56.53, 54.4, 48.85 and 31.0%, respectively. The weight loss in this stage corresponds to the first exotherm in the DTA curves. The DTG maxima of all the metal complexes lie around 300 °C (Table 4).

The activation energies and the frequency factors for the third stage of the thermal degradation, which are due to the oxidation of the charred residue for the various complexes, are given in Table 5. For cotton fibres, a weight loss of 6.45% occurs in the temperature range 410–500 °C with an activation energy of 179.6 kJ mol$^{-1}$. For CSP, the activation energy is reduced to

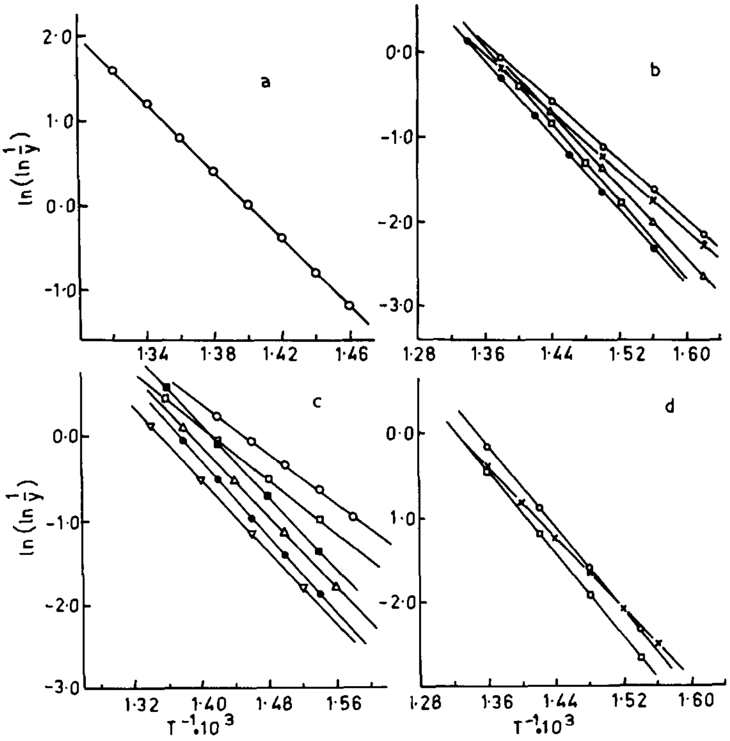

Fig. 6. Plots of $\ln(\ln 1/y)$ vs. $T^{-1} \times 10^3$ using the Broido equation. a, Cotton fibre; b, CSP (●), Ti(III) (○), V(IV) (□), Cr(III) (△) and Mn(II) (×); c, Fe(II) (○), Co(II) (●), Ni(II) (□), Cu(II) (△), Zn(II) (▽) and Zr(IV) (■); d, Mo(VI) (□), Cd(II) (×) and La(III) (○) complexes of CSP for the third stage of the thermal degradation in air.

TABLE 3

Temperature ranges, DTG maxima, activation energies and frequency factors for the first stage of the thermal degradation of cotton fibre, CSP and metal complexes of CSP in air using the Broido method

| Sample No. | Compound/complex | Temperature range (°C) | DTG maxima (°C) | $E_a$ (kJ mol$^{-1}$) | $Z$ (s$^{-1}$) |
|---|---|---|---|---|---|
| 1 | Cotton fibre | 250–285 | – | 178.8 | $1.23\times10^{13}$ |
| 2 | CSP | 100–180 | 106.0 | 43.5 | $2.82\times10^{3}$ |
| 3 | Ti(III)–CSP | 120–190 | 130.0 | 40.3 | $4.0\times10^{2}$ |
| 4 | V(IV)–CSP | 120–200 | 115.0 | 38.5 | $1.43\times10^{2}$ |
| 5 | Cr(III)–CSP | 115–190 | 118.0 | 35.5 | $0.48\times10^{2}$ |
| 6 | Mn(II)–CSP | 110–180 | 135.0 | 45.3 | $1.67\times10^{3}$ |
| 7 | Fe(II)–CSP | 120–190 | 125.0 | 41.0 | $0.7\times10^{3}$ |
| 8 | Co(II)–CSP | 120–190 | 120.0 | 33.5 | $0.4\times10^{2}$ |
| 9 | Ni(II)–CSP | 115–190 | 122.5 | 45.9 | $1.88\times10^{3}$ |
| 10 | Cu(II)–CSP | 115–180 | 115.0 | 40.1 | $2.6\times10^{2}$ |
| 11 | Zn(II)–CSP | 120–200 | 128.0 | 48.2 | $2.97\times10^{3}$ |
| 12 | Zr(IV)–CSP | 120–195 | 130.0 | 36.0 | $0.78\times10^{2}$ |
| 13 | Mo(VI)–CSP | 120–195 | 120.0 | 36.3 | $1.26\times10^{2}$ |
| 14 | Cd(II)–CSP | 115–180 | 122.0 | 46.4 | $1.22\times10^{3}$ |
| 15 | La(III)–CSP | 120–190 | 120.0 | 44.6 | $1.7\times10^{3}$ |

TABLE 4

Temperature ranges, DTG maxima, activation energies and frequency factors for the second stage of thermal degradation of cotton fibre, CSP and metal complexes of CSP in air using the Broido method

| Sample No. | Compound | Temperature range (°C) | DTG maxima (°C) | $E_a$ (kJ mol$^{-1}$) | $Z$ (s$^{-1}$) |
|---|---|---|---|---|---|
| 1 | Cotton fibre | 285–330 | 322.0 | 256.9 | $7.3 \times 10^{20}$ |
| 2 | CSP | 250–300 | 292.0 | 191.8 | $1.97 \times 10^{16}$ |
| 3 | Ti(III)–CSP | 240–300 | 295.0 | 173.1 | $1.85 \times 10^{14}$ |
| 4 | V(IV)–CSP | 245–300 | 295.0 | 187.9 | $4.44 \times 10^{15}$ |
| 5 | Cr(III)–CSP | 240–300 | 285.0 | 188.1 | $7.99 \times 10^{15}$ |
| 6 | Mn(II)–CSP | 250–300 | 305.0 | 159.9 | $3.04 \times 10^{13}$ |
| 7 | Fe(II)–CSP | 240–310 | 310.0 | 175.8 | $9.90 \times 10^{13}$ |
| 8 | Co(II)–CSP | 245–295 | 300.0 | 181.6 | $1.74 \times 10^{14}$ |
| 9 | Ni(II)–CSP | 250–300 | 295.0 | 165.4 | $3.56 \times 10^{13}$ |
| 10 | Cu(II)–CSP | 235–300 | 280.0 | 191.0 | $6.78 \times 10^{15}$ |
| 11 | Zn(II)–CSP | 250–300 | 295.0 | 188.9 | $1.5 \times 10^{15}$ |
| 12 | Zr(IV)–CSP | 240–308 | 305.0 | 169.4 | $4.18 \times 10^{15}$ |
| 13 | Mo(VI)–CSP | 240–300 | 295.0 | 192.1 | $1.26 \times 10^{16}$ |
| 14 | Cd(II)–CSP | 250–300 | 300.0 | 174.0 | $8.61 \times 10^{13}$ |
| 15 | La(III)–CSP | 250–298 | 310.0 | 189.8 | $1.1 \times 10^{15}$ |

TABLE 5

Temperature ranges, DTG maxima, activation energies and frequency factors for the third stage of the thermal degradation of cotton fibre, CSP and metal complexes of CSP in air using the Broido method, and their char yields

| Sample No. | Compound | Temperature range (°C) | DTG maxima (°C) | $E_a$ (kJ mol$^{-1}$) | $Z$ (s$^{-1}$) | Char yield at 700 °C (wt.%) |
|---|---|---|---|---|---|---|
| 1 | Cotton fibre | 410–500 | 412.0 | 179.6 | $0.98 \times 10^{11}$ | 8.8 |
| 2 | CSP | 380–510 | 455.0 | 92.0 | $1.08 \times 10^{4}$ | 25.8 |
| 3 | Ti(III)–CSP | 350–500 | 460.0 | 72.1 | $2.38 \times 10^{4}$ | 24.2 |
| 4 | V(IV)–CSP | 365–500 | 455.0 | 97.2 | $1.52 \times 10^{7}$ | 23.9 |
| 5 | Cr(III)–CSP | 360–520 | 455.0 | 88.7 | $0.77 \times 10^{3}$ | 25.0 |
| 6 | Mn(II)–CSP | 360–500 | 435.0 | 73.7 | $0.52 \times 10^{3}$ | 24.6 |
| 7 | Fe(II)–CSP | 380–520 | 410.0 | 79.4 | $0.5 \times 10^{3}$ | 23.4 |
| 8 | Co(II)–CSP | 370–520 | 455.0 | 93.5 | $1.8 \times 10^{4}$ | 25.7 |
| 9 | Ni(II)–CSP | 350–500 | 470.0 | 66.0 | $0.24 \times 10^{1}$ | 26.9 |
| 10 | Cu(II)–CSP | 380–510 | 410.0 | 88.7 | $6.96 \times 10^{3}$ | 24.6 |
| 11 | Zn(II)–CSP | 350–500 | 444.0 | 83.5 | $0.36 \times 10^{4}$ | 27.9 |
| 12 | Zr(IV)–CSP | 370–500 | 435.0 | 84.5 | $0.56 \times 10^{4}$ | 22.5 |
| 13 | Mo(VI)–CSP | 360–500 | 450.0 | 101.0 | $0.37 \times 10^{5}$ | 22.7 |
| 14 | Cd(II)–CSP | 375–510 | 455.0 | 89.2 | $4.88 \times 10^{3}$ | 25.8 |
| 15 | La(III)–CSP | 350–498 | 435.0 | 99.5 | $0.4 \times 10^{5}$ | 25.2 |

92.0 kJ $mol^{-1}$ with a weight loss of 25.48% in the temperature range 380–510 °C. In the case of metal complexes of CSP, the activation energy and the weight loss lie in the range 73–100 kJ $mol^{-1}$ and 10–22%, respectively, depending upon the metal present. This stage corresponds to the second and third exotherms of the DTA curves. The DTG maxima of all the metal complexes lie around 450 °C (Table 5).

### *Studies of chars*

The char yields (in weight %) of samples 1–15 were obtained from the TG curves at 700 °C and are given in Table 5. The char yield from CSP (25.8%) is much higher than that of cotton fibres (8.8%). This shows that thiophosphorylation lowers the decomposition temperature and the activation energy for the decomposition of cotton fibres and increases the char yield. This observation is supported by DTA and TG studies discussed in the earlier section. The char yields of metal complexes of CSP lie in the range 22.5–25.0%. The char yields are somewhat higher for the Ni(II) and Zn(II) complexes as compared to that of CSP.

### *Spectral studies of chars*

The IR spectra of the chars of CSP and its Fe(II) complex, shown in Figs. 7 and 8, were recorded after subjecting the samples to thermal degradation in air in the temperature range 200–400 °C. The IR spectra of the chars of cotton fibres have been discussed in detail elsewhere [10]. The changes observed in the IR spectra of CSP are as follows. At 200 °C, there is a decrease in the intensity of absorption bands due to hydroxyl stretching and bending (3400, 3300, 1380 and 1320 $cm^{-1}$) along with the bands at 830 (P–O), 780 (P=S) and 680 $cm^{-1}$ (C–Cl). These data strongly indicate the occurrence of dehydration, dethiophosphorylation and dehydrohalogenation reactions. At 260 °C, the band at 1490 $cm^{-1}$ (C=C and C=N vibrations of pyridine) and other normal bands of cellulose partially disappeared. New bands appeared at 1700 (C=O), 1240 (P=O) and 950 $cm^{-1}$ (P–O–P). The band due to P=O can be explained by the following transformation taking place at lower temperature.

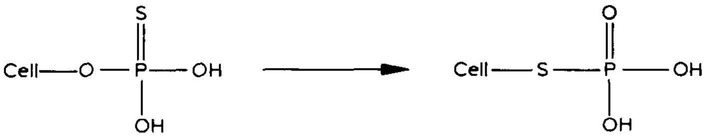

$$\underset{\mathbf{1}}{\text{Cell—O—P(=S)(OH)—OH}} \longrightarrow \underset{\mathbf{2}}{\text{Cell—S—P(=O)(OH)—OH}}$$

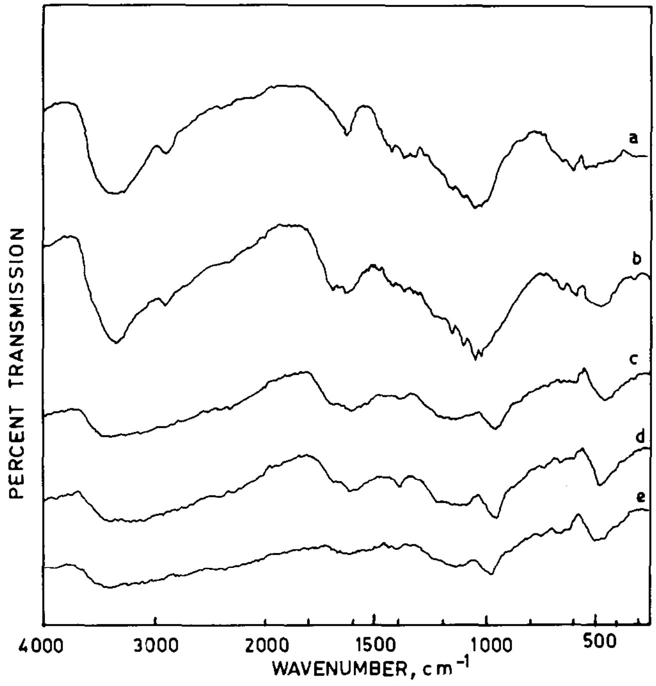

Fig. 7. The IR spectra of (a) CSP and (b–e) chars of CSP prepared at 200, 260, 320 and 400 ° C respectively.

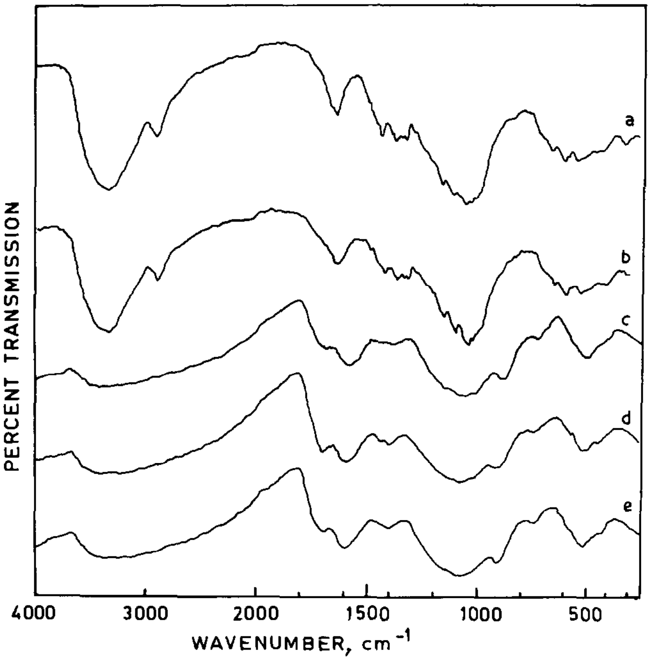

Fig. 8. The IR spectra of (a) the Fe(II)–CSP complex and (b–e) chars of the Fe(II)–CSP complex prepared at 200, 260, 320 and 400 ° C, respectively.

The P–O–P stretch can be explained on the basis that the thiophosphoric acids released during dethiophosphorylation become polymerized. Furthermore, at this temperature the band at 1630 shifts to 1600 $cm^{-1}$ (conjugated C=C). At 320 °C new bands appear at 1400 ($SO_4^{2-}$) [27], 1100 ($PO_4^{3-}$), 1000 (=C–H bending), 900 (P–O–P) and 750 $cm^{-1}$ (P–O). At 400 °C, the normal bands due to cellulose disappeared completely and the bands which appeared at 320 °C, become more intense. The wide band at 950 $cm^{-1}$ explains the formation of many complex organophosphorus compounds. The exact nature of these compounds cannot be explained from this band, but it is of value in quantitative analysis and in the identification of organophosphorus compounds [28].

The changes described above are also observed in the IR spectra of the Fe(II)–CSP complex, the only difference being that the intensity of absorption band at 780 $cm^{-1}$ (P=S) is weak as compared to that of CSP. As there is no appreciable difference between the IR spectra of CSP and its metal complexes, it can be inferred that the basic mechanism of degradation of metal complexes of CSP is the same as that of CSP.

### *ESR spectral studies*

The ESR spectra of cotton fibres, CSP, and the CSP–Fe(II) and CSP–Cu(II) complexes, recorded after heating the samples at 250 °C for 15 min, are shown in Figs. 9 and 10. The $g$ values for these complexes were calculated as 2.035, indicating that the signals in the ESR spectra are due to free radicals. This value is very close to the $g$ value for a free electron [29] which is 2.00232.

In the case of the Fe(II) and Cu(II) complexes, in addition to the signals for free radicals, signals due to paramagnetic $Fe^{2+}$ and $Cu^{2+}$ ions are also observed. However, due to the complexity of the compounds, sharp peaks were not obtained. The relative intensities of the ESR spectral signals were calculated by measuring the peak-to-peak derivative amplitude and peak-to-peak width of the derivative spectral lines using the method described by Wertz and Bolton [29]. The relative intensities correspond to the relative concentration of free radicals [30] formed during the degradation of the samples. The ratios of the concentration of free radicals for cotton fibres, CSP and the CSP complexes with Fe(II) and Cu(II) were found to be 1.0 : 0.41 : 0.1332 : 0.184. Thus the lowest concentration of free radicals formed is in the chars of the Fe(II) complex.

It is obvious that free radicals are formed during the thermal degradation of cotton fibres, CSP and the CSP–metal complexes. Furthermore, the formation of free radicals is much higher in CSP than in the CSP–metal complexes. This is due to the presence of chlorine in CSP, which acts as a flame retardant in the gas phase by forming free radicals. The formation of

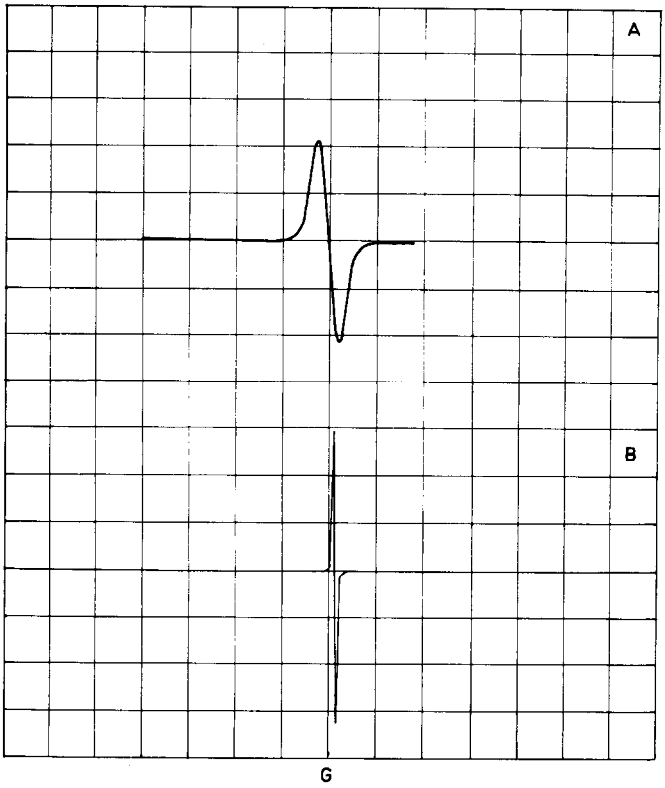

Fig. 9. The ESR spectra of the char of (A) cotton fibre and (B) CSP.

free radicals in the metal complexes may be reduced due to the reaction of the metals with the chlorine to form metal chlorides.

### *Mechanism of thermal degradation*

The mechanism of the thermal degradation of cotton fibres has been reviewed by several workers [19,31–33]. The thermal degradation of CSP starts with the generation of thiophosphoric acid, which then alters the thermal degradation in such a way that the products of laevoglucosan and the other flammable products are minimized [34]. On further heating thiophosphoric acid can polymerize to form polythiophosphoric acid, which is a fairly active catalyst in the dehydration reactions of cellulose. It can react with a cellulose moiety to form CSP, which then breaks down to give water, thiophosphoric acid and the char. This has been discussed in detail by Bhatnagar et al. [35].

As reported by Katsuura and Inagaki [36], during the initial stage of its thermal degradation CSP may be transformed to structure **2** (as shown above) and the mixture of **1** and **2** then degrades at higher temperatures. The

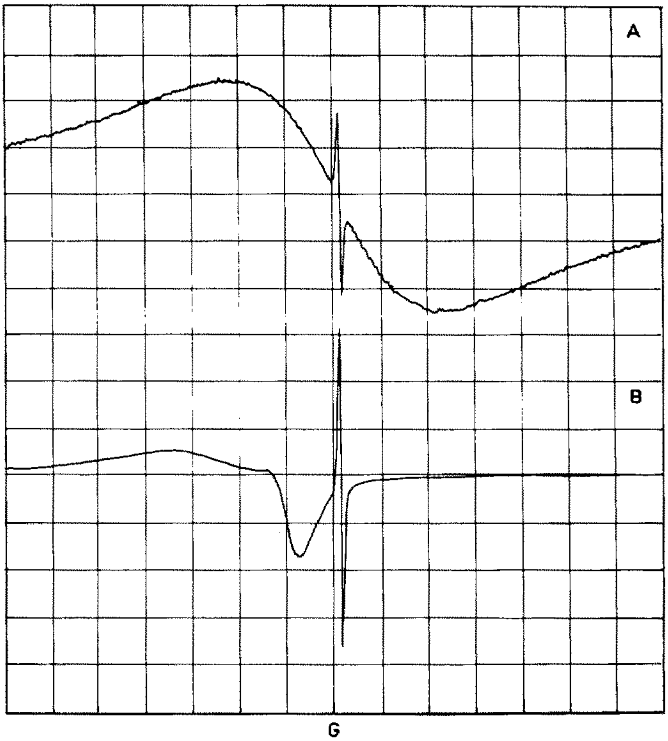

Fig. 10. The ESR spectra of the char of the CSP complexes with (A) Fe(II) and (B) Cu(II).

introduction of sulphur atoms retards the formation of conjugated double bonds by elimination of phosphorus ester groups [37]. Chlorodeoxycellulose is also formed together with CSP. Therefore, the mechanism of the thermal degradation of thiophosphorylated product is also affected by the chlorine content. The first step of the thermal degradation of chlorodeoxycellulose involves the dehydrohalogenation reaction. The released hydrogen chloride catalyses a series of heterolytic reactions, including transglycosylation, dehydration, inter- and intra-molecular etherification, and other condensation reactions that provide laevoglucosenone and other volatile compounds including tarry products. Finally, the homolytic cleavage of the substituents on the carbon chain of the condensation products gives carbonaceous chars still containing trapped and relatively stable free radicals.

In the thermal degradation of the CSP–metal complexes, the first step is dethiophosphorylation, i.e. the removal of the octahedral complex of metal thiophosphates from the cellulose moiety. This complex then decomposes to give a metal thiophosphate of the form $M_x(PSO_3)_y$, and thiophosphoric acid as shown in Scheme 2. The values of $x$ and $y$ depend upon the oxidation number of the cation. Both of the decomposition products can polymerize to form polymetal thiophosphate in metal complexes and polythiophosphoric

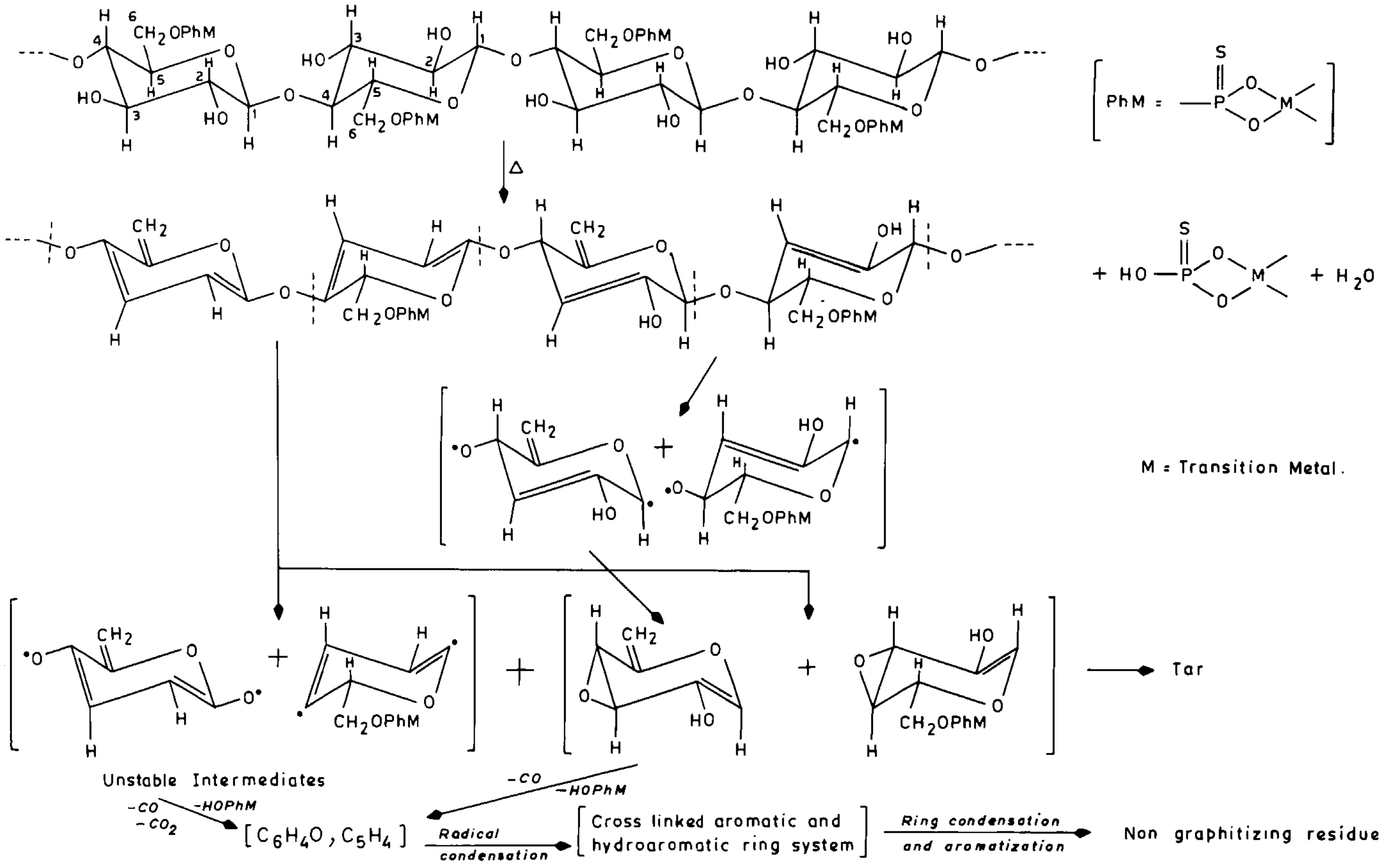

Scheme 2. The thermal degradation of the metal–CSP complexes.

acid in CSP, which, in turn, can react with the cellulose moiety. On further heating, CSP and cellulose metal thiophosphate break down to give water/thiophosphoric acid/metal thiophosphate and dehydrated chars [38].

The thermal degradation of chlorodeoxycellulose present in the metal complexes of CSP takes place in the same manner as described earlier. In the case of the metal complexes of CSP, there is a possibility that hydrogen chloride released in the decomposition of chlorodeoxycellulose may react with the metal ions from the metal thiophosphate to form the metal chloride. The effect of metal chlorides, which are Lewis acids, is similar to that of hydrogen chloride in promoting the dehydration, condensation and charring reactions. Shafizadeh [23] has shown that metal chlorides produce more char and less laevoglucosenone.

## CONCLUSIONS

Cellulose, one of the major textile materials, is intrinsically flammable. Flaming combustion is a gas-phase reaction. In the flaming combustion of cellulose, cellulose first breaks down into smaller volatile fuel compounds, which then volatilize, mix with air and burn. Cellulose is rendered flame resistant by applying a proper condensed-phase active flame retardant, which changes the mechanism of the degradation of cellulose such that the formation of flammable volatile gases is minimized and char formation is increased.

In the present study, lower decomposition temperatures and activation energies of decomposition and higher char yields of cellulose thiophosphate and its metal complexes, as compared to those of cellulose, lead to the conclusion that thiophosphorylation and subsequent complex formation with transition-metal ions is an effective method of imparting flame retardancy to cellulose.

## ACKNOWLEDGEMENTS

This research was financed in part by a grant from the United States Department of Agriculture, Office of International Cooperation and Development, authorised by Public Law 480. One of the authors (R.K.K.) is thankful to this agency for providing a research fellowship.

## REFERENCES

1 H.-G. Elias, Macromolecules, Vol. 2, Plenum Press, New York, 1983, p. 1069.
2 A. Hebeish and J.T. Guthrie, The Chemistry and Technology of Cellulose Copolymers, Springer-Verlag, Berlin, New York, 1981.

3 J.C. Arthur, Jr., Adv. Chem. Ser., 91 (1969) 574.
4 E.H. Immergut, in H.-F. Mark, N.G. Gaylord and N.N. Baker (Eds.), Encyclopedia of Polymer Science and Technology, Vol. 3, Interscience, New York, 1965, p. 247.
5 M.M. Kamel and A. Hebeish, J. Appl. Polym. Sci., 20 (1976) 2407.
6 J. Compton, W.H. Martin and D.M. Gargarine, Text. Res. J., 40 (1970) 813.
7 M.I. Khalil, O.I. Aglan and A. Hebeish, J. Appl. Polym. Sci., 27 (1982) 2377.
8 M.H. El-Rafie, E.M. Khalil, S.A. Abdel-Hafiz and A. Hebeish, J. Appl. Polym. Sci., 28 (1983) 311.
9 D.S. Hon, J. Appl. Polym. Sci., 23 (1979) 359.
10 R.M. Parkins, G.L. Drake, Jr. and W.A. Reeves, J. Appl. Polym. Sci., 10 (1966) 1041.
11 J.E. Hendrix, J.E. Bostic, Jr., E.S. Olson and R.H. Baker, J. Appl. Polym. Sci., 14 (1970) 1701.
12 J.D. Reid and L.W. Mazzeno, Jr., Ind. Eng. Chem., 41 (1949) 2828.
13 B. Kaur, R.K. Jain, I.S. Gur, Hari L. Bhatnagar and H-R. Schulten, J. Anal. Appl. Pyrol., 9 (1986) 173.
14 I.N. Ermolenko, S.S. Gusev and I.P. Lyublinder, Zh. Prikl. Khim., 42 (1969) 2302.
15 B.N. Figgis, Introduction to Ligand Fields, Wiley Eastern Ltd., New Delhi, 1976, pp. 218, 225, 278.
16 J. Lewis and R.G. Wilkins, Modern Co-ordination Chemistry, Interscience, New York, 1967.
17 R.A. Palmer and T.S. Piper, J. Inorg. Chem., 5 (1966) 864.
18 L.F. Larkworthy and K.C. Patel, J. Inorg. Nucl. Chem., 32 (1970) 1264.
19 D. Dollimore and J.M. Hoath, Thermochim. Acta, 5 (1981) 87.
20 E. Shafizadeh, J. Anal. Appl. Pyrol., 3 (1982) 283.
21 J.E. Hendrix and R.H. Barker, Clemson Univ. Rev. Ind. Management Text. Sci., 8 (1969) 63.
22 F. Shafizadeh, Adv. Carbohydr. Chem., 23 (1968) 419.
23 F. Shafizadeh, Appl. Polym. Symp., 28 (1975) 153.
24 W.K. Tang, in R.C. Mackenzie (Ed.), Differential Thermal Analysis, Vol. 2, Academic Press, London, 1972, p. 523.
25 F. Shafizadeh, Y.S. Lai and C.R. McIntyre, J. Appl. Polym. Sci., 22 (1978) 1183.
26 A. Broido, J. Polym. Sci., Part A-2, 7 (1969) 1761.
27 N.B. Colthup, J. Opt. Soc. Am., 40 (1950) 397.
28 L.J. Bellamy, Infrared Spectra of Complex Molecules, Methuen, London, 1958.
29 J.E. Wertz and J.R. Bolton, Electron Spin Resonance, McGraw-Hill, New York, 1972, pp. 12, 32.
30 N-S. Hon, J. Polym. Sci., Polym. Chem. Ed., 13 (1975) 1933.
31 S.L. Madorsky, V.E. Hart and S. Straus, J. Agric. Food Chem., 15 (1967) 773.
32 G.A. Byrne, D. Gardiner and F.H. Holmes, J. Appl. Chem., 16 (1967) 81.
33 K. Kato, Agr. Biol. Chem., 31 (1967) 657.
34 J.W. Lyons, J. Fire Flammability, 1 (1970) 302.
35 R.K. Jain, K. Lal and Hari L. Bhatnagar, J. Appl. Polym. Sci., 30 (1985) 897.
36 K. Katsuura and N. Inagaki, J. Appl. Polym. Sci., 22 (1978) 679.
37 K. Katsuura and N. Inagaki, Text Res. J., 45 (1975) 103.
38 B. Kaur, I.S. Gur and Hari L. Bhatnagar, J. Appl. Polym. Sci., 31 (1986) 667.